Lattice-Distortion Engineering of Zero-Dimensional Metal Halide Single Crystal for High-Performance Scintillator

*Xin Chen[1], Zehui Xiang[2], Jian Chen[2], Fansheng Meng[4], Yunzhong Zhu[1, *], Wei Wang[1, 3, *]*

[1] Sino-French Institute of Nuclear Engineering and Technology, Sun Yat-sen University, Zhuhai 519082, P. R. China

[2] School of Physics and Astronomy, Sun Yat-sen University, Zhuhai 519082, P. R. China

[3] School of Physics, Sun Yat-sen University, Guangzhou, 510275, P. R. China

[4] School of Materials Science and Engineering, Liaocheng University, Liaocheng, P. R. China

[*]Corresponding author

zhuyzh7@mail.sysu.edu.cn (Yunzhong Zhu)

wangw223@mail.sysu.edu.cn (Wei Wang)

Calculation method

The calculation formula for the deformation index D value is as follows:

$$D = \frac{1}{n}\sum_{i=1}^{n}\left|\frac{l_i - l_{ave}}{l_{ave}}\right| \#(1)$$

Here, n represents the coordination number of the central cation, li is the bond length between each coordinating anion and cation, and lave is the average bond length. The calculation formulas for the radiation recombination rate (K_r) and the non-radiation recombination rate (K_{nr}) are as follows:

$$K_r = \frac{PLQY}{\tau} \#(2)$$

$$K_{nr} = \frac{1 - PLQY}{\tau} \#(3)$$

The improved Arrhenius equation proposed by Shibata is as follows:

$$I(T) = I_0 \frac{1 + Aexp\left(-\frac{E_a}{k_B T}\right)}{1 + Bexp\left(-\frac{E_b}{k_B T}\right)} \#(4)$$

Among them, I(T) and I_0 represent the PL integral intensities at temperature T and 0 K respectively. k_B is the Boltzmann constant, E_a indicates the thermal activation process initiated by the shallow energy level intermediate state, and E_b corresponds to the activation energy of the non-radiative recombination channel at high temperatures. A and B are the coefficients related to the negative thermal quenching and thermal quenching processes respectively.

Scintillator

The scintillation detector system is mainly composed of Hamamatsu R6231-100 photomultiplier tube (PMT), SHR high-voltage power supply, custom pre-amplifier circuit board, CAKE611 shaping amplifier, RIGOL DP831A DC power supply, and Pico Scope 5000 data acquisition system. Before the test, the single crystal is wrapped with polytetrafluoroethylene tape to reduce light scattering, and only the light-emitting surface is retained to obtain the encapsulated scintillation body. Then, an appropriate amount of optical silicone oil is applied to the photomultiplier tube window to achieve optical coupling with the scintillation body. The negative high voltage used in the test is 900V. All data are processed using MATLAB R2024a software. After performing Gaussian fitting on the universal peak, the energy resolution is calculated using the ratio of full width at full width at half maximum (FWHM) to the corresponding channel number.

The relative light output of the scintillator was calibrated using the standard commercial scintillator NaI. The calculation formula is as follows:

$$LY_{Sample} = \frac{H_{sample} \cdot \beta_{Sample}}{H_{NaI} \cdot \beta_{NaI}} LY_{NaI} \#(5)$$

Where LY, H, β is the light yield, channel number and external quantum efficiency, respectively.

The relationship between the energy resolution of the scintillator and the gamma-ray energy can be fitted using the following empirical formula:

$$ER = \left(a + \frac{b}{\sqrt{E_\gamma}}\right) \#（6）$$

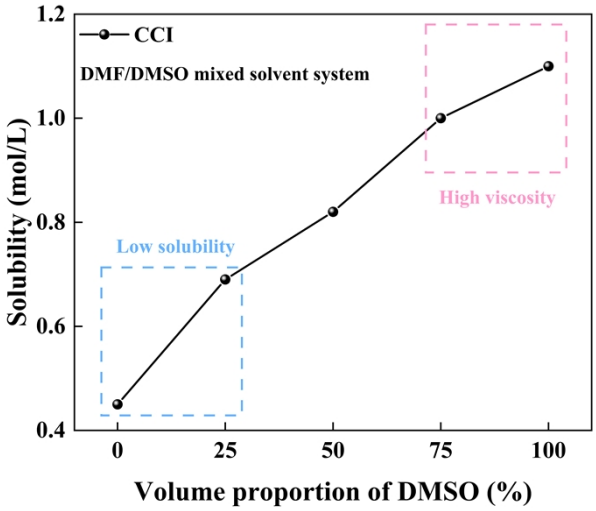

Figure S1. CCI precursor solubility curves under different volume proportion of DMSO.

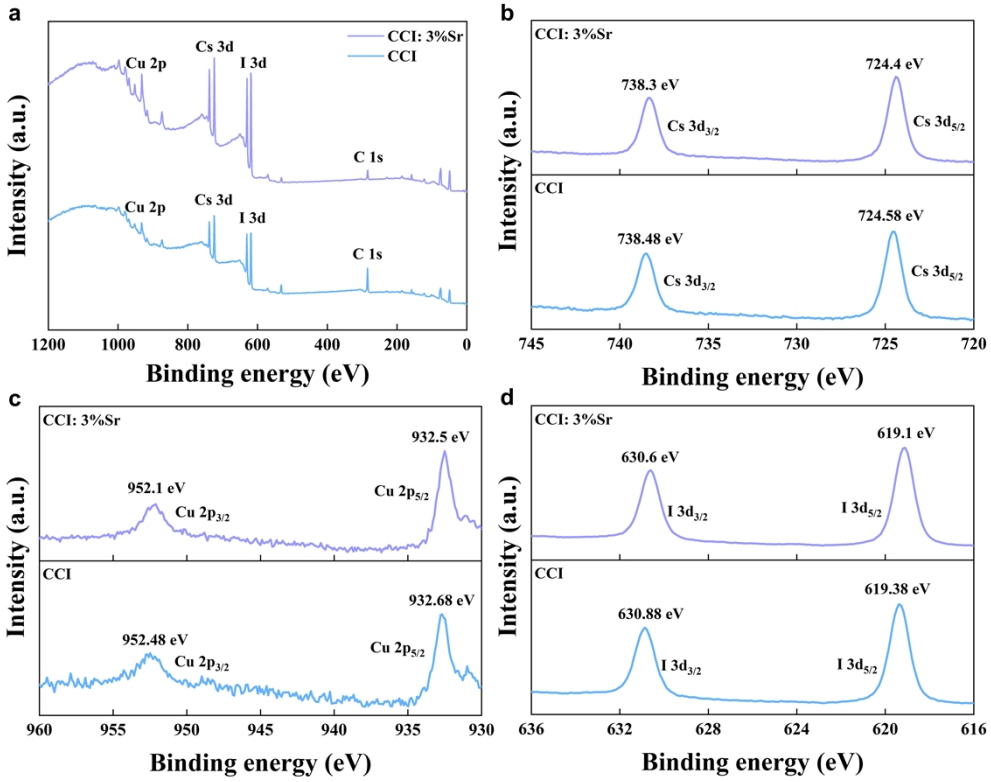

Figure S2. (a) XPS full spectra of CCI and CCI: 3%Sr single crystals. (b-d) XPS spectra of Cs 3d, Cu 2p, and I 3d in CCI and CCI: 3%Sr.

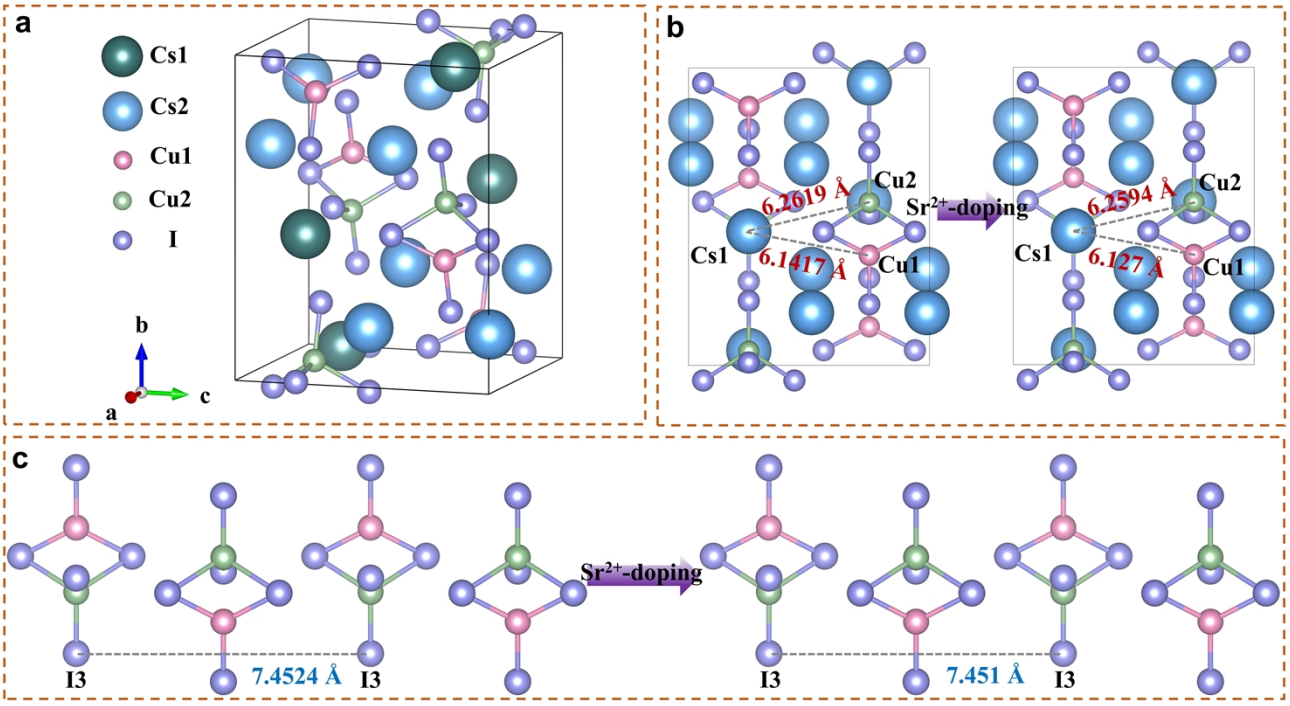

Figure S3. (a) Crystal structure model of CCI. (b) Comparison of Cs1-Cu1/Cu2 distances after 3% Sr^{2+} doping. (c) Comparison of I3-I3 distances between adjacent unit cells.

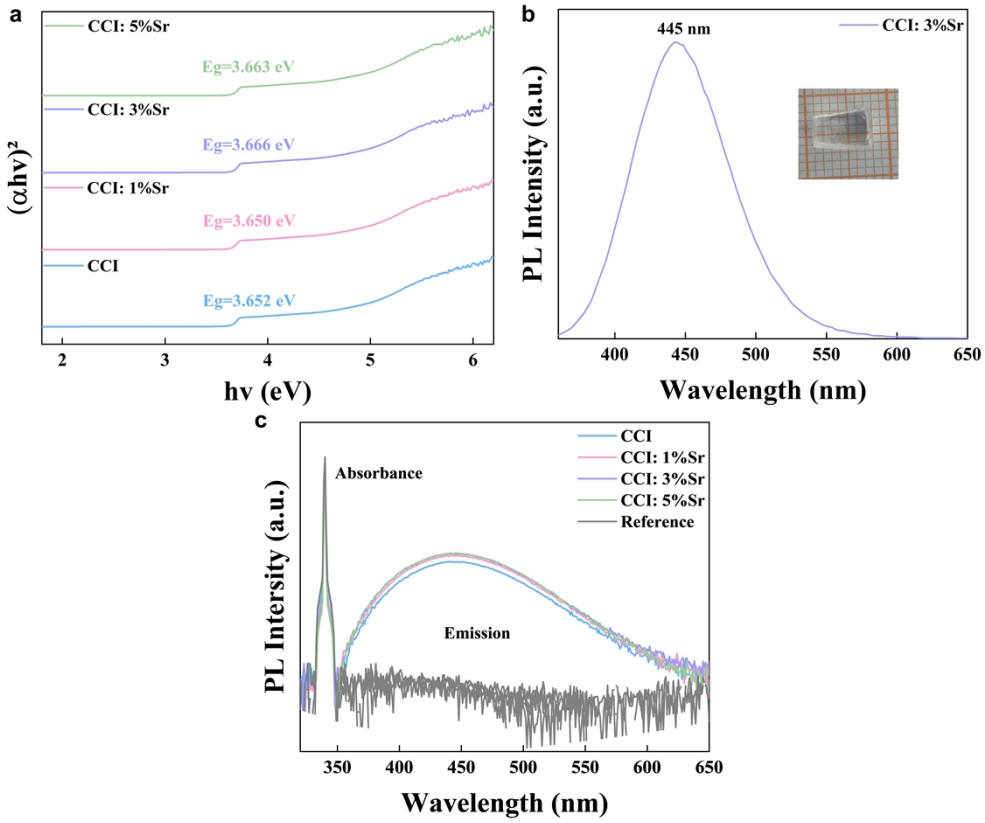

Figure S4. (a) Tauc curve of CCI: x%Sr single crystals. (b) The photograph of CCI: 3%Sr single crystal after grinding and polishing treatment and corresponding PL spectra. (c) PLQY measurement results of CCI: x%Sr single crystals.

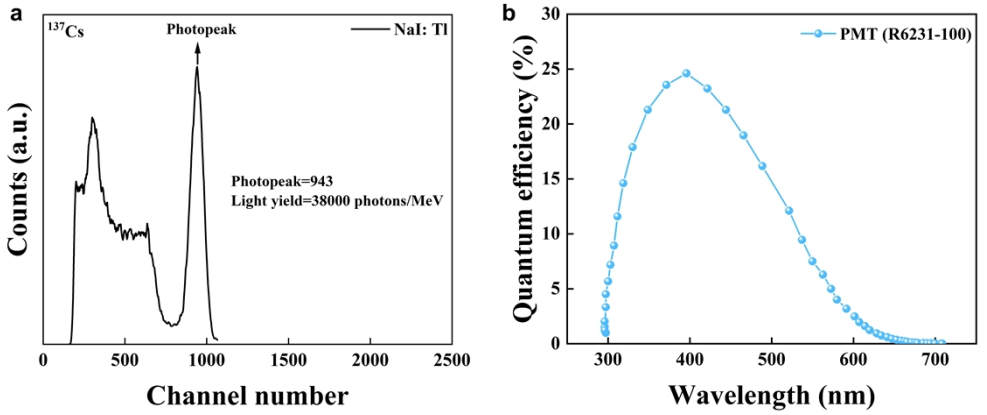

Figure S5. (a) The pulse height spectrum of the NaI: Tl scintillator under the ^{137}Cs radiation source. (b) The external quantum efficiency curve of the photomultiplier tube (R6231-100).

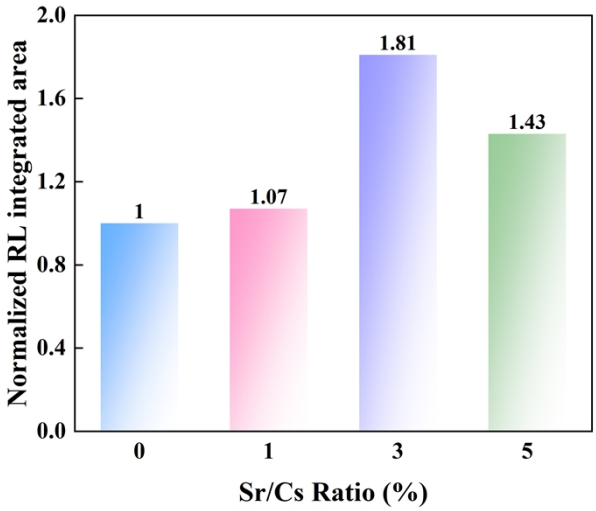

Figure S6. Normalized RL integrated area of CCI: x%Sr single crystals.

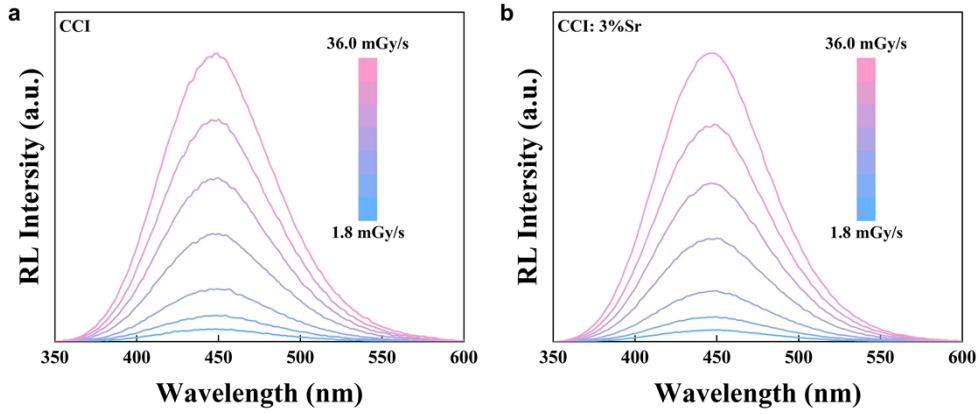

Figure S7. RL spectra of (a) CCI and (b) CCI: 3%Sr single crystals under different X-ray dose rates.

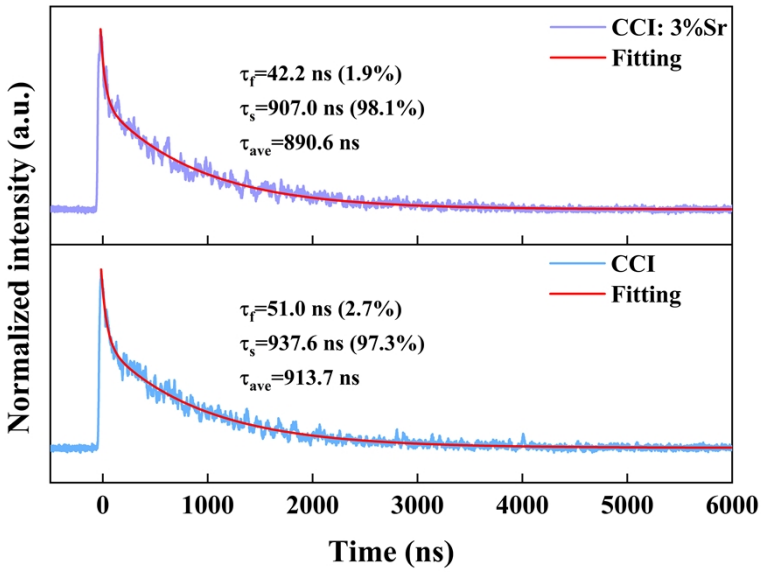

Figure S8. The scintillation decay curves of pure CCI and CCI: 3%Sr single crystals under ^{137}Cs radiation source.

Table S1. Crystal structure data for pure CCI and CCI: 3%Sr crystals.

Empirical formula	CCI	CCI: 3%Sr
Formula weight/g·mol^{-1}	1160.31	1160.31
Crystal system	orthorhombic	orthorhombic
Space group	Pnma	Pnma
a/Å	10.1000(3)	10.1027(2)
b/Å	11.5824(3)	11.5773(3)
c/Å	14.2881(3)	14.2861(4)
α/°	90	90
β/°	90	90
γ/°	90	90
Volume/Å^3	1671.45(7)	1670.93(7)
Z	4	4
Density/g·cm$_{-3}$	4.611	4.612
M/mm^{-1}	18.176	18.181
F(000)	1952	1952

Table S2. Calculated recombination rate of radiation and non-radiation.

CCI: x%Sr	PLQY (%)	τ (ns)	Kr (×10^{-5} s^{-1})	Knr (×10^{-5} s^{-1})
0	76.74	1005.2	7.6343	2.3139
1	79.48	940.4	8.4517	2.1821
3	83.81	982.9	8.5268	1.6472
5	81.68	991.5	8.2380	1.8477

Table S3. Detailed parameters of energy resolution calculation.

Materials	Source Energy (keV)	W	Xc	FWHM(=$\sqrt{ln4}$W≈1.1774W)	Energy resolution (%)
CCI	662	51.07±3.51	953	60.13±4.13	6.31±0.43
CCI: 1%Sr	662	48.93±3.44	1026	57.61±4.05	5.62±0.39
CCI: 3%Sr	662	45.71±2.73	1083	53.82±3.21	4.97±0.30
CCI: 5%Sr	662	53.82±4.53	1052	63.37±5.33	6.02±0.50
CCI	511	41.59±4.87	725	48.97±5.73	6.75±0.79
CCI: 3%Sr	511	38.98±2.02	828	45.90±2.38	5.54±0.29
CCI	1275	72.74±14.82	1756	85.64±17.45	4.88±0.99
CCI: 3%Sr	1275	60.13±6.41	2012	70.80±7.55	3.52±0.38
CCI	356	32.65±2.56	507	38.44±3.01	7.58±0.59
CCI: 3%Sr	356	31.28±2.61	577	36.83±3.07	6.38±0.53
CCI	344	33.14±4.93	487	39.02±5.80	8.01±1.19
CCI: 3%Sr	344	30.73±3.13	553	36.18±3.69	6.54±0.67
CCI	244	27.62±6.65	352	32.52±7.83	9.24±2.22
CCI: 3%Sr	244	25.12±3.51	399	29.58±4.13	7.41±1.04
CCI	122	17.03±0.56	189	20.05±0.66	10.61±0.35
CCI: 3%Sr	122	16.60±0.54	213	19.54±0.64	9.17±0.30
CCI	59.5	13.03±0.22	101	15.34±0.26	15.19±0.26
CCI: 3%Sr	59.5	12.86±0.22	112	15.14±0.26	13.52±0.23

Table S4. Light yield calculation parameters.

Materials	Wavelength (nm)	EQE (%) (R6231-100)	Channel number	Light yield (photons/MeV)
NaI: Tl	415	23.57	943	38000

CCI	448	20.88	953	43400
CCI: 1%Sr	448	20.88	1026	46700
CCI: 3%Sr	448	20.88	1083	49300
CCI: 5%Sr	448	20.88	1052	47900

Table S5. Performance comparison of CCI series single-crystal scintillators.

Materials	Growth Method	Preprocess	Wavelength (nm)	^{137}Cs Energy resolution (%)	Light yield (photons/Mev)	Ref.
$CsCu_2I_3$	Solution	No need	576	11.6	20000	[1]
$CsCu_2I_3$	Bridgman	Cut and polish	575	10.5	10248	[2]
$CsCu_2I_3$: 5%Li			575	6.8	10900	
$CsCu_2I_3$: 3%Na	Bridgman	Cut and polish	575	9.3	9376	[3]
$Cs_3Cu_2I_5$	Bridgman	Cut and polish	445	7.19	24000	[4]
$Cs_3Cu_2I_5$: 1%Li			445	5.25	28000	
$Cs_3Cu_2I_5$: 0.5Tl	Bridgman	Cut and polish	505	4.8	83000	[5]
$Cs_3Cu_2I_5$	Solution	Cut and polish	444	5.6	38000	[6]
$Cs_3Cu_2I_5$	Bridgman	Cut and polish	452	7.7	18000	[7]
$Cs_3Cu_2I_5$: 1%Tl			517	4.5	51000	
$Cs_3Cu_2I_5$	Solution	Polish	445	6.89	31418	[8]
$Cs_3Cu_2I_5$: 5%Na			445	5.37	34707	
CCI	Solution	No need	448	6.31	43350	This work
CCI: 3%Sr			448	4.97	49264	

References

1. B. Bansal, V. Anand, N. K. Tailor, V. Ranga, S. Satapathi, P. J. Sellin, M. Tyagi and G. Anil Kumar, *IEEE Transactions on Nuclear Science*, 2025, **72**, 3169-3177.
2. D. Liu, Q. Wei, Y. Tong, P. Xiang, P. Cai, G. Tang, H. Shi and L. Qin, *CrystEngComm*, 2023, **25**, 58-63.
3. C. Shu, Q. Wei, D. Liu, W. Li, H. Yin, H. Li, G. Tang and L. Qin, *Crystals*, 2023, **13**, 1157.
4. P. Xiang, Q. Wei, C. Wang, P. Cai, Y. Tong, G. Tang, X. Sun, F. Yang, H. Shi, Z. Liu and L. Qin, *Journal of Materials Chemistry C*, 2022, **10**, 15400-15407.
5. R. Zheng, L. Wang, Y. Liu, J. Chen, P. Xiao and Q. Xie, *Journal of Crystal Growth*, 2024, **627**, 127512.
6. Y. Li, H. Shen, Y. Li, Y. Gu, J. Zhao, L. Li and J. Xu, *Ceramics International*, 2024, **50**, 32603-32612.
7. D. Yuan, *ACS Applied Materials & Interfaces*, 2020, **12**, 38333-38340.
8. Y. Lei, L. Xu, Y. Wang, L. Lian, C. Liu, Y. Wang, L. Liang, Z. Qin, S. Han, W. Zheng, Q. Hu, X. Liu, T. Wang and W. Jie, *Journal of Materials Chemistry A*, 2025, **13**, 22660-22671.